

Structural and elastic properties of a confined 2D colloidal solid: a molecular dynamics study

M. Ebrahim Foulaadvand^{1,2} and Neda Ojaghloou¹
foolad@iasbs.ac.ir

¹ Department of Physics, University of Zanjan, P. O. Box 45196-313, Zanjan, Iran

² School of Nano-science, Institute for Research in Fundamental Sciences (IPM) , P.O. Box 19395-5531, Teheran, Iran

(Dated: June 16, 2021)

We implement molecular dynamics simulations in canonical ensemble to study the effect of confinement on a $2d$ crystal of point particles interacting with an inverse power law potential proportional to r^{-12} in a narrow channel. This system can describe colloidal particles at the air-water interface. It is shown that the system characteristics depend sensitively on the boundary conditions at the two *walls* providing the confinement. The walls exert perpendicular forces on their adjacent particles. The potential between walls and particles varies as the inverse power of ten. Structural quantities such as density profile, structure factor and orientational order parameter are computed. It is shown that orientational order persists near the walls even at temperatures where the system in the bulk is in fluid state. The dependence of elastic constants, stress tensor elements, shear and bulk moduli on density as well as the channel width is discussed. Moreover, the effect of channel incommensurability with the triangular lattice structure is discussed. It is shown that incommensurability notably affects the system properties. We compare our findings to those obtained by Monte Carlo simulations and also to the case with the periodic boundary condition along the channel width. .

PACS numbers:

I. INTRODUCTION

Colloidal crystals are a valuable model system, since the effective interactions between colloidal particles can be manipulated to a large extent. Furthermore, convenient techniques to observe the structure and dynamics of such systems are available [1–5]. Colloidal dispersions under geometric confinement can serve us to understand the effects of confinement on the ordering of various types of nanoparticles. Related phenomena occur in a wide variety of systems, e.g.; electrons at the surface of liquid helium that is confined in a quasi-one-dimensional channel [6], dusty plasmas [7]; hard disks [8, 9] and magnetorheological [10] colloids under confinement which are of great interest for various microfluidic and other applications. Two-dimensional colloidal dispersions have been used successfully in studies on melting in two dimensions during the last decades [11–13]. In previous studies, much attention has been paid to the generic effect of confinement on crystalline order in $d = 2$ and to the extent and range over which the confining boundaries disturb (or enhance, respectively) the degree of order. The effect of external walls on phase behavior has been studied for a long time [14, 15]. The confining wall can cause structural transition such as layering transition [16–19]. Another interesting aspect of confinement is related to formation of extended defects, solitonic staircase and standing strain wave superstructures [20–23]. In this paper we intend to gain a more insight and shed more lights onto a previously studied problem which is a two dimensional confined colloidal system between two walls which exert forces on the particles [24]. We implement molecular dynamics simulation and compare our findings to those obtained earlier by Monte Carlo simulations [24].

II. DESCRIPTION OF THE PROBLEM

Consider a $2d$ system of zero size soft disks, i.e.; point particles, interacting under a purely repulsive force with the inverse power law potential $U(r) = \epsilon(\frac{\sigma}{r})^p$ where r denotes the distance between particles. The motivation for taking the spatial dimension $d = 2$ comes from experimental fact that some colloidal particles with super paramagnetic cores in the interface of water-air thin film can be described by a $2d$ system of particles interacting with the above repulsive potential with $p = 3$ [21, 25]. However, the exponent p is taken to be 12 for computational convenience in our paper. We recall that taking $p = 3$ makes the potential long range which is computationally inconvenient and needs special treatment. Choosing $p = 12$ has the merit that we can compare our findings with the bulk results obtained by extensive simulations [26]. We have chosen the cutoff distance $r_c = 3\sigma$ and has adopted a reduced system of units in which ϵ and σ are taken as unity ($k_B = 1$). Now we discuss how to represent the effect of confining walls. One choice is to take a smooth repulsive wall located at $x = x_{wall}$, described by a wall potential [27] $U_{wall} = \epsilon_{wall}(\frac{\sigma}{|x-x_{wall}|})^{10}$. The motivation for a decay with the 10th power is the idea that such a potential would result if we have a semi infinite crystal with a power law interaction given by the above equation, but no cutoff, and the total potential is summed over the half space [27]. We initially set the particles on the sites of a triangular lattice which is confined between a two dimensional channel. The channel walls are taken to be along the y direction having a distance D from each other. The system length along the y direction is L and periodic boundary condition is applied in the y direction. The particles number is shown by N and the

number density is given by $\rho = \frac{N}{A}$ in which $A = DL$ is the channel area. Let a_0 denotes the lattice constant in the triangular lattice (distance between nearest neighbours). The relation between ρ and a_0 is given by $\rho^{-1} = \frac{\sqrt{3}a_0^2}{2}$. Figure (1) illustrates the choice of the geometry: the left wall lies at $x = 0$ and the right wall is located at $x = D$.

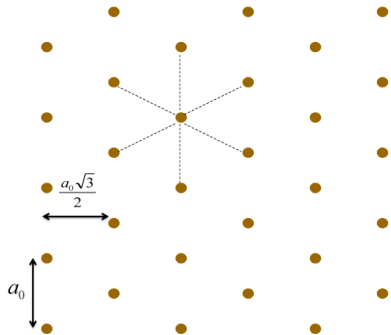


FIG. 1: Geometry of the problem. A 2D colloidal solid with triangular lattice structure is confined between two walls. The particles exert repulsive forces between each other. Lattice spacing is a_0 .

We remark that one can place a triangular configuration of particles between confining walls in two different methods. In the first method, two of the six nearest neighbours of each particle are located northward and southward of it whereas in the second method two of the six nearest neighbours are located westwards and eastwards. These two configurations are mapped into each other by a ninety degree rotation (see figure two). As we shall see in the rest of the paper, the elastic properties of the confined colloidal solid differs notably for these configurations. We show the distance between the first (last) column of particles from the left (right) wall by d_L (d_R) respectively. The number of columns (rows) are denoted by N_c and N_r correspondingly. Note the number of particles is given by $N = N_c N_r$. In our simulations, we mainly have chosen $D = (N_c + 1) \frac{\sqrt{3}a_0}{2}$ with $d_L = d_R = \frac{\sqrt{3}a_0}{2}$ but we have also studied the incommensurate case where $D \neq (N_c + 1) \frac{\sqrt{3}a_0}{2}$ ($d_L \neq d_R$). In our simulations we have chosen $\epsilon_{wall} = 0.0005$ unless otherwise stated. It has been shown that by this choice, the distance between columns coincide, within error, with the ideal value $\frac{\sqrt{3}}{2}a_0$. The readers can refer to [24] for the further details.

A. Simulation method and details

We have employed molecular dynamics in the NEV ensemble to simulate the model in the reduced units. We remark that the initial velocities are such chosen to give

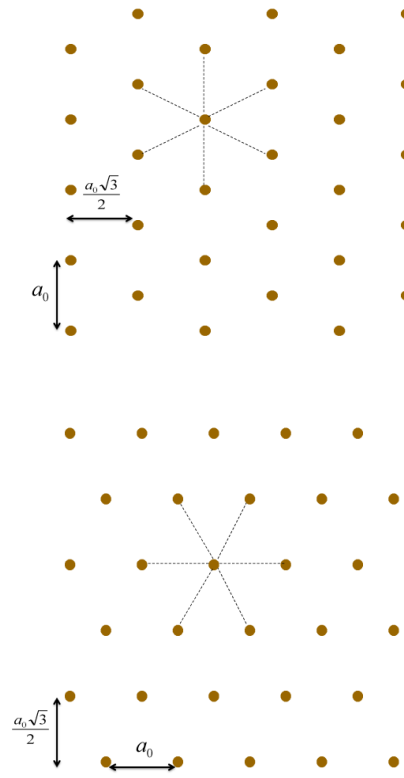


FIG. 2: Two methods of placing particles between the confining walls. In method one, two of the six nearest neighbours are located upward and downward to the central particle (main figure). In method two (which is rotated by ninety degree) two of the six nearest neighbours are located leftwards and rightwards to the central particle (upper right corner figure).

rise to the desired temperature when the system reaches to a steady state. The simulation parameters and details are as follows. The velocity Verlet algorithm has been used for integrating the equations of motion with a time step of $\Delta t = 0.01$, the number of simulation timestep has been mainly chosen $T = 10^6$ where 2×10^5 time steps are discarded for equilibration. The cut off radius $r_c = 3\sigma$ and the shifted-force potential has been taken into account.

III. STRUCTURAL PROPERTIES

In this section we present our simulation results for a narrow channel. Figure (3) shows the profile of density at two temperatures with soft wall boundary condition with $N_c = 20$ and $N_r = 120$ for the method one of initial triangular setting of particles. For comparison the result for a system with periodic boundary condition (PBC) along the x direction is shown as well. The temperature $k_B T = 1$ is below the melting point for both soft walls and PBC whereas at $k_B T = 3$ the PBC system seems

to be melted but the soft wall system is not melted yet. You see in the soft wall system, the presence of confining walls enhances the density profile near the walls. Similar phenomenon is observed in the Monte Carlo simulation of the problem [24].

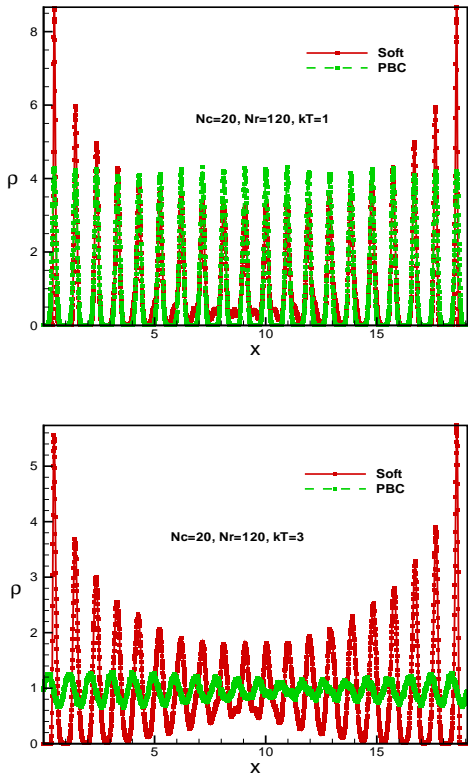


FIG. 3: Density profile for a narrow channel with $N_c = 20$ and $N_r = 120$ at two different temperatures. Both boundary conditions soft wall (methods one) and periodic are sketched. Top: $k_B T = 1$, bottom: $k_B T = 3$.

In figure (4) we compare the density profiles for methods one and two for the same temperatures as in figure (3). At low temperatures the results are close to each other and there is no qualitative difference. When the temperature is raised to $k_B T = 3$ the difference between two methods becomes noticeable. Near walls the density profile is the same but when we leave the walls and approach the centre, the method two system melts easier than the method one system. This suggests that method one system is more stiff and exhibits a higher persistence to melting rather than method two system. The reason is due to the number of particles per unit length in the adjacent column to the walls. In method one this number is proportional to $\frac{1}{a_0}$ whereas in method two this number is proportional to $\frac{1}{\sqrt{3}a_0}$ which is smaller. Consequently in method two the force per unit length exerted by a wall to its adjacent column of particles is smaller.

In figure (5) the density profiles for a temperature above the melting points for both methods one and two

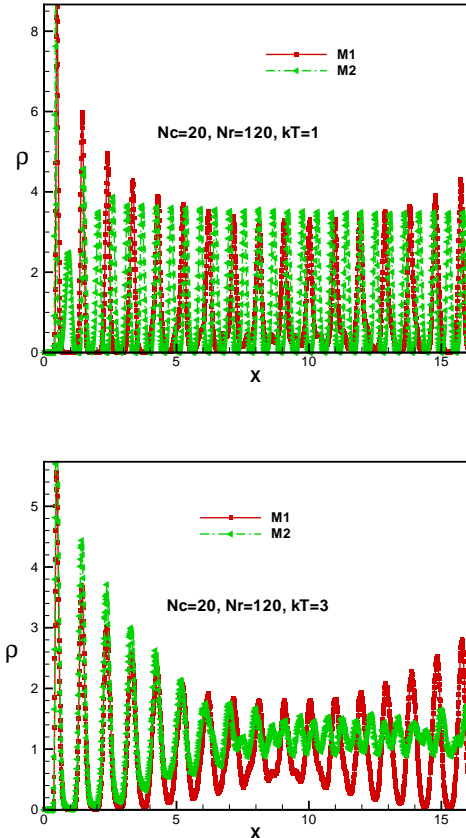


FIG. 4: Density profile for a narrow channel with $N_c = 20$ and $N_r = 120$ at two different temperatures. Soft wall boundary condition with both methods one and two is considered. Top: $k_B T = 1$, bottom: $k_B T = 3$.

as well as PBC are shown. Note in the soft wall boundary condition, the system favours to preserve its layering structure near the walls. In the soft wall boundary condition the profiles of method one and two are almost similar to each other. As stated earlier, in method two, the melting in the centre is more evident.

Next we exhibit the structure factor $S(\mathbf{q})$ in figure (6) for a temperature below the melting point where the colloidal system is in the solid phase. The boundary condition is soft walls. We recall the definition of the structure factor $S(\mathbf{q})$:

$$S(\mathbf{q}) = \frac{1}{N} \sum_{l,m} \langle e^{i\mathbf{q} \cdot (\mathbf{r}_l - \mathbf{r}_m)} \rangle \quad (1)$$

Where $\langle \rangle$ denotes time averaging. We show this quantity for both methods of initial setting. Note in method one we have taken $\mathbf{q} = (q, 0)$ whereas in method two we took $\mathbf{q} = (0, q)$. The sharp peaks confirm the solid structure of the system. The first (largest) peak is associated with the nearest neighbour distance a_0 .

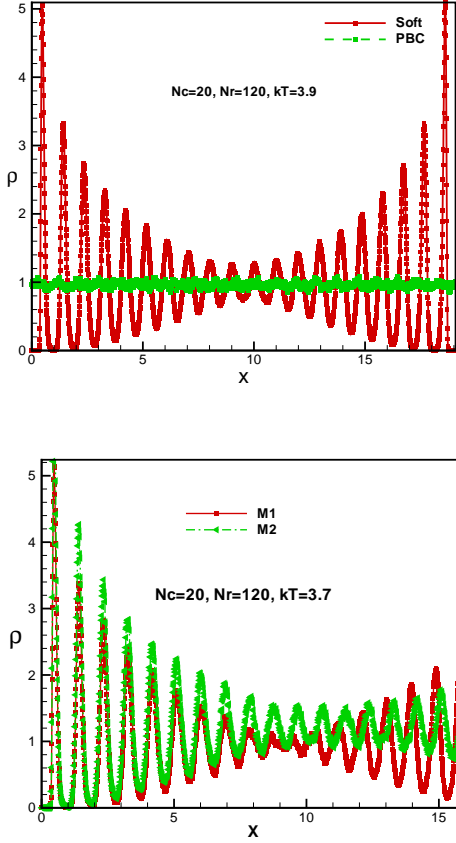


FIG. 5: Top : Density profile for a narrow channel with $N_c = 20$ and $N_r = 120$ at a temperature above the melting point for both boundary conditions soft wall and periodic. bottom: comparison of methods one and two in soft wall boundary condition.

To give a quantitative description of the degree of order in the system, we obtain the orientational order parameter Ψ_6 . This quantity is related to the local orientational order parameter associated with each particle k .

$$\Psi_6(k) = \frac{1}{6} \sum_{j(\text{n.n. of } k)} e^{6i\phi_{jk}} \quad (2)$$

Where ϕ_{jk} denotes the angle between a reference line (here positive y axis) and the line connecting particle k to particle j . Figure (7) shows the profile of orientational order parameter squared modulus for a narrow channel at various temperatures at $\rho = 1.05$ for the soft wall system. As you can see the modulus of Ψ_6 is greater near walls than in the channel centre. Similar to density profile, the walls enhance the degree of orientational order near them. The results of Monte Carlo simulations show quite similar behaviour [24]. As you can see there is notable difference between methods one and two of initial triangular setting at high temperatures. Method one has higher orientational order than method two which can

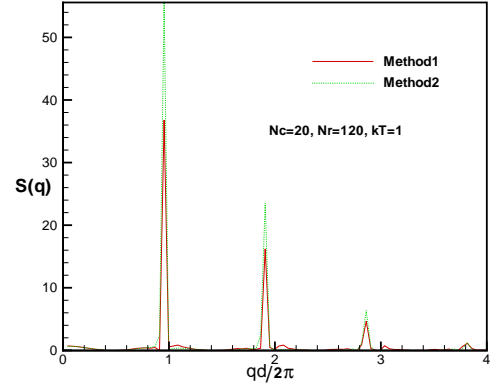


FIG. 6: Structure factor $S(q)$ for a narrow channel with soft wall boundary condition at a temperature $k_B T = 1$ for initial setting. Methods one and two give identical results.

be attributed to its higher stiffness. The difference gets sharper when the temperature arises.

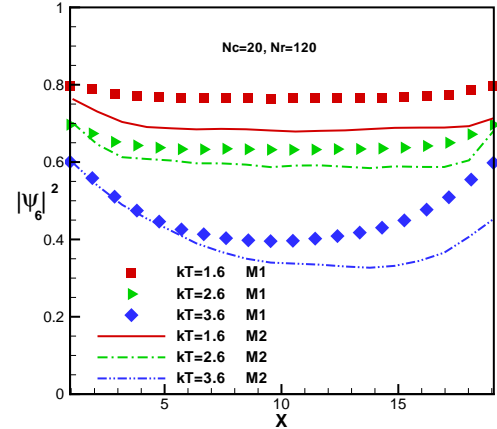


FIG. 7: The squared modulus of the orientational order parameter profile Ψ_6 of a narrow channel with soft-wall boundary condition at $\rho = 1.05$ for various values of temperature. Methods one and two are shown.

Figure (8) shows the dependence of the orientational order parameter squared modulus at the channel centre as well as near its walls versus T at $\rho = 1.05$ for both methods one and two. These results are in qualitative agreement with MC results [24]. When the vicinity of the walls are considered only a monotonous decrease with the temperature is observed. On the contrary, when the channel centre is considered, a change in the slope emerges which can be attributed to system melting in the centre. By increasing the temperature, the difference between methods one and two becomes enhanced.

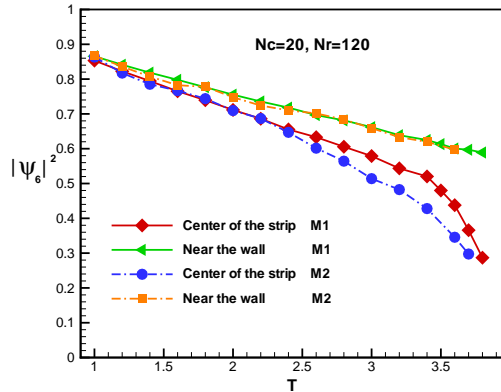


FIG. 8: Temperature dependence of the orientational order parameter squared modulus at the centre as well as near the channel walls. Method one and two are compared to each other.

IV. ELASTIC CONSTANTS

Apart from the study of the lattice structure, positional and orientational order parameters and structural properties, there is also considerable interest in the mechanical properties and in particular elastic constants of two-dimensional crystals. The dependence of these elastic constants on temperature (or density, respectively) plays a crucial role in the theory of two-dimensional melting [13, 28, 29]. One expects a significant effect of the symmetry of the crystal structure. The Voigt notation has been implemented here [30]. In $2d$ we have four elastic constants $C_{11}, C_{22}, C_{12}, C_{33}$. In this paper we have implemented the method of stress fluctuation to obtain the elastic constants [31, 32]. This method which is based on an atomic-level description was originally introduced by Born and Huang [33]. The contribution from the particles to the elastic constants are as follows :

$$C_{\alpha\beta\gamma\delta}(i) = \frac{1}{2\Omega(i)} \sum_{j \neq i} \left(\frac{\phi''(r_{ij})}{r_{ij}^2} - \frac{\phi'(r_{ij})}{r_{ij}^3} \right) [x_\alpha(j) - x_\alpha(i)] \times [x_\beta(j) - x_\beta(i)] [x_\gamma(j) - x_\gamma(i)] [x_\delta(j) - x_\delta(i)] + \frac{\phi'(r_{ij})}{r_{ij}} [x_\beta(j) - x_\beta(i)] [x_\gamma(j) - x_\gamma(i)] \delta_{\alpha\delta} \quad (3)$$

Note the term proportional to $\delta_{\alpha\delta}$ should not be considered in the soft wall case. The contribution from a wall is obtained from the following relation:

$$C_{\alpha\beta\gamma\delta}(i) = \frac{1}{2\Omega(i)} \left[\frac{1}{x_i^2} \phi''_W(x_i) - \frac{1}{x_i^3} \phi'_W(x_i) \right] [x_\alpha^W - x_\alpha(i)]$$

$$[x_\beta^W - x_\beta(i)] [x_\gamma^W - x_\gamma(i)] [x_\lambda^W - x_\lambda(i)] \quad (4)$$

In which ϕ_W is the wall potential imposed on the particles. Also note $x_y^W = y_i$ and $x_x^W = 0$ for the left wall and $x_x^W = D$ for the right wall. Figure (9) shows the dependence of elastic constants in a narrow channel versus the density in the solid phase. Soft wall boundary condition is implemented and both methods of initial triangular setting are considered. All the components increase with increment of ρ . This seems natural since the solid becomes more tough when the density is increased. Except C_{11} for which both methods give identical results, the other three components of the elastic tensor shows notable difference for method one and two. For C_{12} and C_{33} the method two has higher value in a given density whereas for C_{22} method one value is larger than method two.

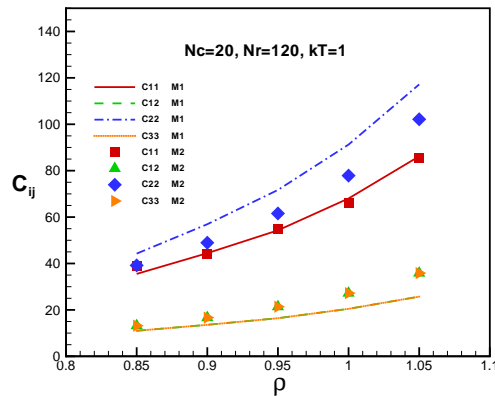


FIG. 9: Dependence of the elasticity tensor components on density in soft wall boundary condition at $k_B T = 1$ for both methods one and two. The values of the elastic constants show substantial difference in methods one and two.

In order to have a further insight into the problem, we have investigated the dependence of elastic constants at a give density ($\rho = 1.05$) on the channel width D . Figure (10) exhibits the dependence of elastic constants on the number of columns N_c and the rows N_r .

The channel width $D = (N_c + 1) \frac{\sqrt{3}a_0}{2}$ plays a noticeable role. The constant C_{11} is mostly affected by the channel width. C_{22} has leastly affected. After N_c increases beyond 60 (which equals to $\frac{N_r}{2}$) the channel width D plays almost no role and the values approach the bulk ones. Our result in figure (10a) are in qualitative agreement with those by monte Carlo simulations [24]. The main difference is that in our results, C_{12} and C_{33} coincide with each other when the system width becomes large whereas in [24] they do not. Notice the symmetry $C_{12} = C_{33}$ is expected in the bulk. The values of our elastic constants are less than those in [24]. We remark that the channel length in reference [24] ($N_r = 30$) is not the same as ours ($N_r = 120$). Similar to previous graph, for C_{11} methods one and two give almost identi-

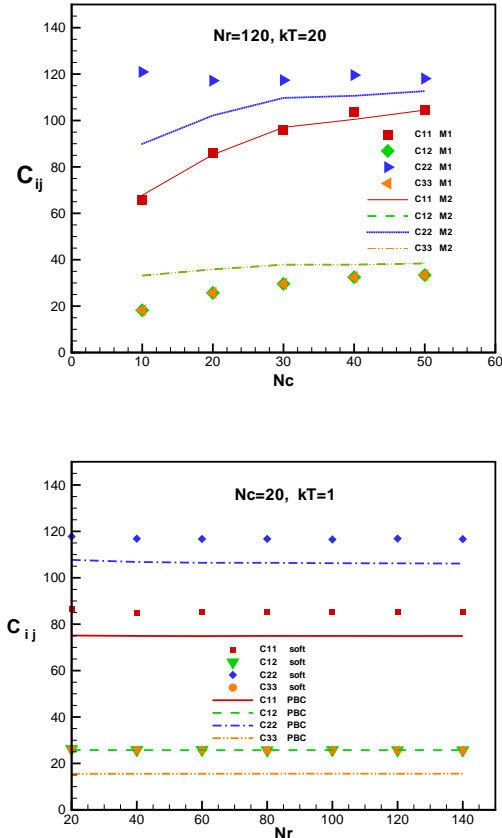


FIG. 10: Top: Dependence of the elasticity tensor components on the number of columns N_c for the soft wall system at $k_B T = 1$ for both methods one and two. bottom: dependence of the elastic tensor components on the number of rows N_r for both soft wall (method one) and periodic boundary condition at $k_B T = 1$. The value for the elasticity tensor components in the PBC are smaller than the corresponding values in the soft wall boundary condition.

cal results. Also for a given width D , C_{12} and C_{33} are larger for two while C_{22} is smaller. Molecular dynamics simulation allows us to compute the components of the stress tensor by averaging over the system particles trajectories. The stress tensor elements can, in principle, be evaluated from the particles trajectories. There are two contributions: one from the particles and other one from the walls. The contribution from the particles to the stress tensor component associated to particle i turns out to be [32]:

$$\sigma_{\alpha\beta}(i) = \frac{1}{2\Omega(i)} \sum_{j \neq i} \frac{1}{r_{ij}} \phi'(r_{ij}) [x_\alpha(j) - x_\alpha(i)] [x_\beta(j) - x_\beta(i)] \quad (5)$$

To evaluate the wall contribution, we assume each wall as a fixed particle with infinite mass at the same height of particle i . With this in mind, the contribution of the left wall which is located at $x_{LW} = 0$ becomes:

$$\sigma_{\alpha\beta}^{LW}(i) = \frac{1}{2\Omega(i)} \phi'_{LW}(x_i) \delta_{\alpha,x} x_\beta(i) \quad (6)$$

In which $\phi_{LW}(x_i)$ is the potential energy between the left wall and particle i . Similarly, the contribution from the right wall yields to be:

$$\sigma_{\alpha\beta}^{RW}(i) = \frac{1}{2\Omega(i)} \phi'_{RW}(D - x_i) \delta_{\alpha,x} (D - x_\beta(i)) \quad (7)$$

Dependence of the stress tensor components on the density for a temperature below melting is shown in figure (11).

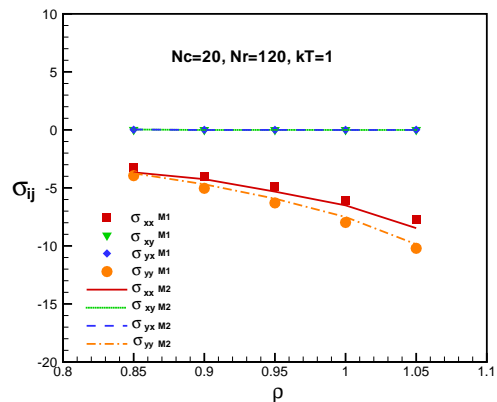


FIG. 11: Dependence of the stress tensor components on the density for a narrow channel with soft wall boundary condition in the solid phase (method one and two are exhibited).

As can be seen, the symmetry $\sigma_{xy} = \sigma_{yx}$ is fulfilled. There is a notable dependence for the nonzero components σ_{xx} and σ_{yy} on the density. By increasing the density ρ , they tend to decrease. As you can see there is not much difference between method one and two. In figure (12) we have sketched the dependence of bulk and shear moduli B and μ on ρ and N_c for a narrow channel with soft wall boundary condition for methods one and two. These quantities increase non linearly with the density ρ . Again we see that beyond $N_c = \frac{N_r}{2}$ there is almost no dependence on N_c . In comparison between methods one and two, we see that the bulk modulus does not show significant change but the shear modulus does. In fact, method two gives larger shear modulus which is expected since method two system has a smaller degree of stiffness and hence larger shear modulus.

V. CHANNEL WITH INCOMMENSURATE WIDTH TO TRIANGULAR LATTICE

In the previous sections, the channel width D was carefully chosen such that the ideal triangular lattice structure fits into the channel as perfectly as possible. It

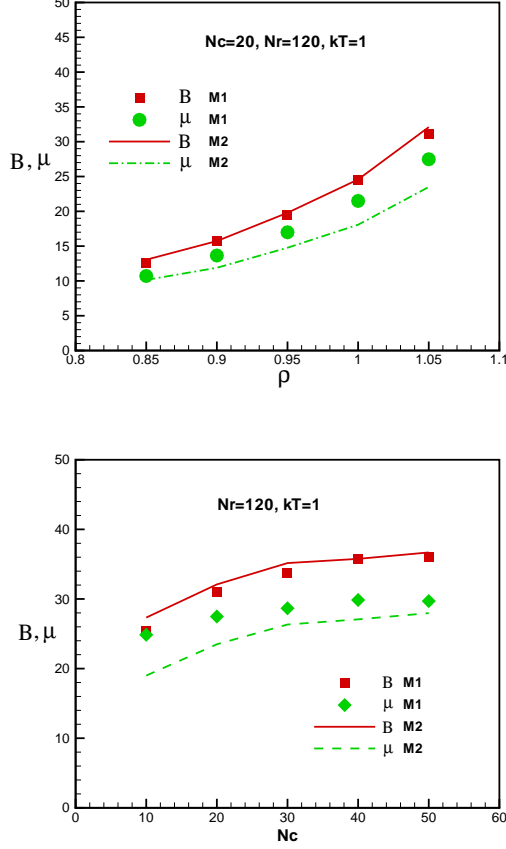


FIG. 12: Top: Density dependence of the bulk and shear moduli B and μ in the solid phase soft wall boundary condition. Bottom: Column number dependence of the bulk and shear moduli B and μ in the solid phase. Methods one and two are compared.

would be interesting to see what happens when such a choice is not made, and D does not correspond to an integer multiple of the distance between columns $d = \frac{\sqrt{3}a_0}{2}$ (method one). Such questions have been considered in the literature (e.g., Refs. [24]) for ultra thin strips and structures rather rich in defects were found. Here we investigate the impact of the incommensurability on the system characteristics. Figures (13) and (14) show the dependence of stress and elasticity tensors components on the incommensurability parameter Δ which is defined as $d_R = \frac{\sqrt{3}a_0}{2} + \Delta$. We observe the bulk and shear moduli are mostly affected by variations of Δ whereas stress and elasticity components are less affected. In figure (13) we see that σ_{xy} and σ_{yx} do not show any significant dependence on Δ whereas the diagonal elements σ_{xx} and σ_{yy} exhibit quite noticeable dependence on Δ . In figure (14) we observe that in the incommensurate system the elasticity tensor components decrease when Δ is increased.

Eventually in figure (15) we have shown the dependence of bulk and shear moduli on Δ . Similar to elas-

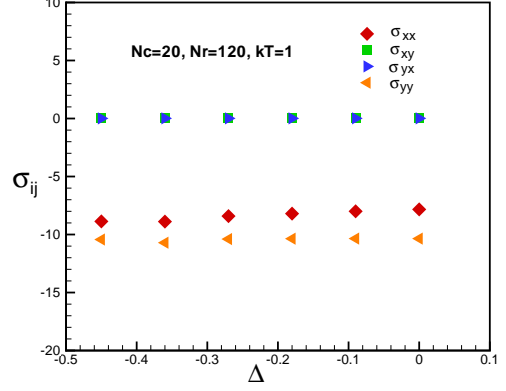


FIG. 13: Dependence of the stress tensor components on the incommensurability parameter Δ . The results are for the method one of the soft wall boundary condition.

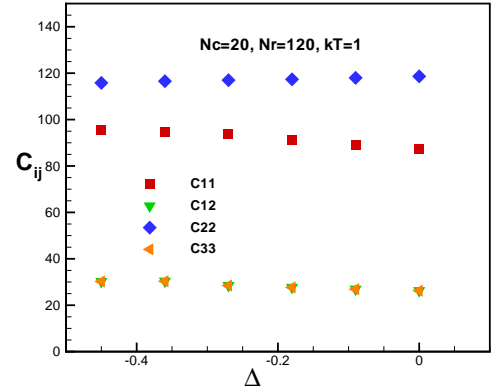


FIG. 14: Dependence of the elasticity tensor components on the incommensurability parameter Δ for the method one.

ticity tensor, by increasing the degree of incommensurability the bulk and shear moduli decrease. The amount of decrease is quite sharp.

VI. SUMMARY AND CONCLUSION

We have used molecular dynamics simulations to study the effect of confinement on a $2d$ crystalline solid, with triangular structure, of point particles interacting with an inverse power law potential proportional to r^{-12} in a narrow channel. Two methods of initial setting of particles in a triangular lattice is discussed. The system characteristics depend sensitively on the interaction of the two walls providing the confinement. The walls exerts perpendicular forces on their adjacent particles. Some structural quantities namely density profile, structure factor and orientational order parameter are computed and their dependence on temperature, density and

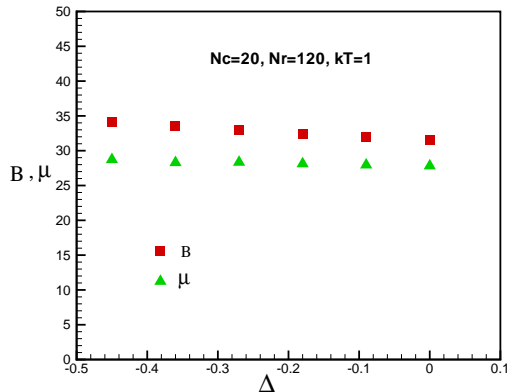


FIG. 15: Dependence of B and μ on the incommensurability parameter Δ for the method one.

other system parameters are evaluated. It is shown that orientational order persists near the walls even at temperatures where the system in the bulk is in the fluid state. Moreover, the dependence of elastic constants, stress ten-

sor elements, shear and bulk moduli on density as well as the channel width is discussed and is shown they increase with raising the density. The effect of varying the channel width is explored and it is found that in general the bulk and shear moduli increase with increasing the channel width until the width becomes comparable to the system length. Furthermore, the effect of incommensurability of the channel with the triangular lattice structure is discussed. It is shown that incommensurability notably affects the system properties. We compare our findings to those obtained by Monte Carlo simulations in [24] and also to the periodic boundary condition along the channel. .

VII. ACKNOWLEDGEMENT

We are highly indebted to Professor Surajit Sengupta for his valuable comments and fruitful discussions. We wish to express our gratitude to Prof. Hashem Raffi Tabar and Dr Abbas Montazeri for their useful helps and enlightening discussions. M.E.F is thankful to No'rooz Khan for his valuable discussions. .

-
- [1] W. C. Poon and P. N. Pusey, in *Observation, Prediction and Simulation of Phase Transitions in Complex Fluids*, edited by M. Baus, F. Rull, and J. P. Ryckaert (Kluwer, Dordrecht, 1995), p. 3.
- [2] H. Löwen *J. Phys.: Condens. Matter* **13**, R415 (2001).
- [3] *Coloidal Dispersions in External Fields* edited by H. Löwen and C. N. Likos, special issue of *J. Phys.: Condens. Matter* **16**, No. 38 (2004).
- [4] P. N. Pusey, in *Liquids, Freezing and the Glass Transition*, edited by J. P. Hansen, D. Levesque and J. Zinn-Justin (North Holland, Amsterdam, 1991).
- [5] K. Zahn, A. Wille, G. Marert, S. Sengupta and P. Nielaba, *Phys. Rev. Lett.* **90**, 155506 (2003).
- [6] P. Glasson, V. Dotsenko, P. Fozooni, M. J. Lea, W. Bailey, G. Papageorgiou, S. E. Andresen, and A. Kristensen, *Phys. Rev. Lett.* **87**, 176802 (2001).
- [7] Y.-L. Lai and Lin I, *Phys. Rev. E* **64**, 015601(R) (2001).
- [8] P. Pieranski et al., *Mol. Phys.* **40**, 225 (1980).
- [9] D. Chaudhuri and S. Sengupta, *Phys. Rev. Lett.* **93**, 115702 (2004).
- [10] R. Haghgoie and P. S. Doyle, *Phys. Rev. E* **70**, 061408 (2004).
- [11] K. J. Strandburg, *Rev. Mod. Phys.* **60**, 161 (1988); **61**, 747 (1989).
- [12] S. Sengupta, P. Nielaba, and K. Binder, *Phys. Rev. E* **61**, 6294 (2000).
- [13] K. Binder, S. Sengupta, and P. Nielaba, *J. Phys.: Condens. Matter* **14**, 2323 (2002).
- [14] K. Binder and P. C. Hohenberg, *Phys. Rev. B* **6**, 3461 (1972); **9**, 2194 (1974).
- [15] K. Binder, in *Phase Transitions and Critical Phenomena*, Vol. 8, edited by C. Domb and J. L. Lebowitz (Academic, London, 1983), p.1.
- [16] P.G. de Gennes, *Langmuir* **6**, 1448 (1990).
- [17] J. Gao, W. D. Luedtke and U. Landman, *Phys. Rev. Lett.* **79**, 705 (1997).
- [18] A. Chaudhuri, S. Sengupta and M. Rao, *Phys. Rev. Lett.* **95**, 266103 (2005).
- [19] D. Chaudhuri, S. Sengupta, *J Chem. Phys.* **128**, 194702 (2008).
- [20] A. Blaaderen *Prog. Colloid Polym. Sci.* **104**, 59 (1997).
- [21] K. Zahn and G. Maret, *Phys. Rev. Lett.* **85**, 3656 (2000).
- [22] G. Piacente, I. V. Schweigert, J. j. Betouras and F. M. Peeters, *Phys. Rev. B* **69**, 045324 (2004).
- [23] Y. H. Chui, S. Sengupta, I. K. Snook and K. Binder *J. chem. Phys.* **132**, 074701 (2010).
- [24] A. Ricci, P. Nielaba, S. Sengupta, and K. Binder, *Phys. Rev. E* **75**, 011405 (2007).
- [25] K. Zahn, J. M. Mendez-Alcaraz, and G. Maret, *Phys. Rev. Lett.* **79**, 175 (1997).
- [26] K. Bagchi, H. C. Andersen, and W. Swope, *Phys. Rev. E* **53**, 3794 (1996).
- [27] P. Nielaba, K. Binder, D. Chaudhuri, K. Franzrahe, P. Henseler, M. Lohrer, A. Ricci, S. Sengupta, and W. Strepp, *J. Phys.: Condens. Matter* **16**, S4115 (2004).
- [28] B. I. Halperin and D. R. Nelson, *Phys. Rev. Lett.* **41**, 121 (1978).
- [29] A. P. Young, *Phys. Rev. B* **19**, 1855 (1979).
- [30] P. M. Chaikin and T. C. Lubensky, *Principles of Condensed Matter Physics* (Cambridge University Press, Cambridge, England, 1995).
- [31] D.R. Squire, A. C. Holt and W. G. Hoover, *Physica* (Amsterdam), **42**, 388 (1969).
- [32] H. Raffi-Tabar, *Phys. Report* **390** (2004).
- [33] M. Born and k. huang, *Dynamical Theory of Crystal Lattices*, Clarendon Press, Oxford (1954).